Int. J. Heat Mass Transfer. Vol. 29, No. 2, pp. 193–201, 1986
Printed in Great Britain

0017–9310/86 $3.00 + 0.00
Pergamon Press Ltd.

The onset of natural convection in a fluid layer suddenly heated from below

KYOUNG-HOON KIM* and MOON-UHN KIM†

Departments of * Mechanical Engineering and † Applied Mathematics, Korea Advanced Institute of Science and Technology, P.O. Box 150, Chongyangni, Seoul, Korea

(*Received* 22 *April* 1985 *and in final form* 29 *July* 1985)

Abstract—The onset of convection in a fluid layer in which the temperature profile is developing in time is considered with inclusion of random fluctuations when a constant heat flux is suddenly applied to the bottom surface. Using the expansion in terms of the eigenfunctions of the linear instability, the governing equations are reduced to a set of ordinary random differential equations, which are solved by a Monte Carlo simulation. The dependency of the onset time of convection on the Rayleigh number and the Prandtl number is investigated. Numerical results are in good agreement with available experimental data.

1. INTRODUCTION

WHEN AN initially quiescent fluid layer is heated from below (or cooled from above) with the corresponding Rayleigh number exceeding a critical value, the quiescent state breaks down and convection sets in. The instability of a fluid layer with time-dependent temperature profile has received considerable attention. One of the most important problems for the stability of a fluid layer heated in a time-dependent manner is to find the time at which the convection is initiated.

Lick [1] and Currie [2] analysed the stability of a fluid layer with the base temperature varying in time by adopting a quasi-steady model, in which the base state is frozen at each instant in time. Homsy [3] and Wankat and Homsy [4] determined a lower bound to the onset time by means of the energy method. In these methods the time appears only parametrically and the onset of convection is treated by modifying the stability analysis of the fluid layer with time-independent temperature profiles. Calculated onset times are, in general, considerably lower than experimental observations. Another approach for the determination of the onset time is to integrate directly the time-dependent equations (initial value techniques) [5–7]. In this method the onset time of convection is taken to be when the fastest growing disturbance has increased to a suitable factor of its initial magnitude. However, the result shows a marked sensitivity to initial data, and to fit experimental data values of the amplification factor ranging several orders are necessary [6]. Another theoretical weakness lies in the assumption that the disturbances are present only at the initial instant.

Recently, onset of convection from random fluctuations has been investigated for stress-free boundaries subject to step and linear changes in surface temperature by Jhaveri and Homsy [8] and for rigid boundaries subject to various prescribed changes in surface temperature by the present authors [9]. The advantages of introducing random forcing are that it immediately specifies the status of initial values and that it takes into consideration continuous presence of noise during the evolution.

Many investigations concerned with the experimental determination of the onset time have been reported in the literature [10–15]. Nielsen and Sabersky [14] carried out transient experiments in which the motion was driven by a constant heat flux at the lower surface. They examined the effects of different heating rates on the onset of convection, on the change of Rayleigh number with time and on the development of motion subsequent to the onset of instability.

In this study we consider the onset of convection when an initially isothermal fluid layer confined by two rigid horizontal surfaces is heated with a constant heat flux at the lower surface while the upper surface is held at the initial temperature. Effects of random fluctuations on the determination of the onset time are included. Special attention is paid to the effects of heating rates and fluid properties on the onset of convection.

2. ANALYSIS

Consider an initially quiescent and isothermal Boussinesq fluid layer confined between two rigid plates which are infinitely extended in horizontal directions. At the instant $\tilde{t} = 0$, a constant heat flux Q is applied to the lower surface, while the upper surface temperature is maintained at the initial temperature T_0.

After introducing the following dimensionless variables

$$x_i = \tilde{x}_i/h, \quad u_i = \tilde{u}_i h/\kappa, \quad t = \tilde{t}\kappa/h^2,$$

$$p = (\tilde{p} - \rho_0 g\tilde{z})h^2/\mu\kappa, \quad T = (\tilde{T} - T_0)k/hQ,$$

the governing equations with inclusion of random fluctuations may be written in the dimensionless form as [16]:

$$\frac{\partial u_j}{\partial x_j} = 0, \tag{1}$$

NOMENCLATURE

a dimensionless wavenumber
$a_m(t), b_m(t), c_m(t), d_m(t)$ amplitudes of the variables
$A_{mn}, B_{mn}, C_{mn}, I^l_{mn}, J^l_{mn}$ dimensionless coefficients
$B_m(t)$ Wiener process
D differentiation with respect to z
$f(z,t), f_n(t)$ random forcing term
g gravitational acceleration
h fluid depth
H dimensionless heat flux
$\mathrm{Im}(\cdot)$ imaginary part of $(\cdot)$
k thermal conductivity
L differential operator, D^2-a^2
Nu Nusselt number, H/R
p pressure
Pr Prandtl number
Q heat flux at lower surface
R Rayleigh number based on ΔT, $\alpha g \Delta T h^3/\kappa\nu$
$\mathrm{Re}(\cdot)$ real part of $(\cdot)$
s surface temperature shape factor, $\int_0^{t_c} \Delta T(t)\,dt/\Delta T(t_c)t_c$
s_{ij} random stress tensor
t time
T temperature
T_0 initial temperature
T_{cond} conductive temperature
ΔT temperature difference between the surfaces
u_i, u, v, w velocity components
$W(z,t)$ Fourier amplitude
x_i, x, y, z rectangular coordinates.

Greek symbols

α thermal expansion coefficient
δ Dirac delta function
δ_{mn} Kronecker delta
ε $Pr\, a^3\theta/\pi$
θ intensity of random forcing
$\Theta(z,t), \Theta_0(z,t)$ Fourier amplitudes
κ thermal diffusivity
λ_n eigenvalue of $\phi_n(z)$
μ viscosity
ν kinematic viscosity
ρ density
ρ_0 density at the initial temperature
$\phi_n(z)$ eigenfunctions satisfying equations (16) and (17).

Subscripts

c quantity at onset of convection
sc quantity of stationary critical condition.

Other symbols

$\tilde{}$ dimensional quantity
$\langle\ \rangle$ ensemble average.

$$\frac{1}{Pr}\left(\frac{\partial u_i}{\partial t}+u_j\frac{\partial u_i}{\partial x_j}\right) = -\frac{\partial p}{\partial x_i}+HT\delta_{i3}+\frac{\partial^2 u_i}{\partial x_j \partial x_j}+\frac{\partial s_{ij}}{\partial x_j}, \quad (2)$$

$$\frac{\partial T}{\partial t}+u_j\frac{\partial T}{\partial x_j}=\frac{\partial^2 T}{\partial x_j \partial x_j}. \quad (3)$$

Here the coordinate $x_3(=z)$ is measured vertically upwards from the lower surface, $H=\alpha g Q h^4/\kappa\nu k$ denotes the dimensionless heat flux at the lower surface and $Pr=\nu/\kappa$ the Prandtl number. s_{ij} is the Gaussian random stress tensor in thermodynamic fashion, statistical correlations of which are given as:

$$\langle s_{ij}\rangle = 0,$$
$$\langle s_{ij}(x_p,t_1)s_{lm}(x_q,t_2)\rangle = 2Pr\,\theta\delta(x_p-x_q)\delta(t_2-t_1)\times(\delta_{il}\delta_{jm}+\delta_{im}\delta_{jl}). \quad (4)$$

In (3) we have neglected the random heat flux vector which is much smaller than the random stress tensor for most fluids [8]. Neglecting the fluctuations at the boundaries, the boundary conditions are

$$u_i=0,\quad \frac{\partial T}{\partial z}=-1 \text{ at } z=0,$$
$$u_i=0,\quad T=0 \text{ at } z=1. \quad (5)$$

At the initial stage it is expected that no convection will occur and that heat will be transferred only by conduction. The conductive temperature $T_{cond}(z,t)$ satisfies

$$\frac{\partial T_{cond}}{\partial t}=\frac{\partial^2 T_{cond}}{\partial z^2} \quad \text{for} \quad t\geqslant 0,\quad 0<z<1 \quad (6)$$

with the initial and boundary conditions

$$T_{cond}(z,t)=0 \quad \text{for} \quad t<0,$$
$$\frac{\partial T_{cond}}{\partial z}(0,t)=-1,\quad T_{cond}(1,t)=0 \quad \text{for} \quad t\geqslant 0. \quad (7)$$

The solution of equation (6) satisfying (7) is

$$T_{cond}(z,t)=1-z-2\sum_{n=1}^{\infty}\frac{e^{-\mu_n^2 t}}{\mu_n^2}\cos\mu_n z, \quad (8)$$
$$\mu_n=\left(n-\frac{1}{2}\right)\pi.$$

For the analysis of transient convection, following Jhaveri and Homsy [8], we assume that the first convective motion appears in a two-dimensional form, large-scale features of convective motion at onset are dominated by one horizontal mode and the mean-field approximation is applicable. Thus we restrict our analysis to two dimensions and retain only one mode in the horizontal structure when the variables are decomposed. In addition, the dimensionless number θ giving the variance of the random stress is assumed to be constant in time.

With these assumptions, the Fourier decomposition of the dependent variables in the horizontal direction can be written as

$$w(x,z,t) = W(z,t)\cos ax, \tag{9}$$

$$T(x,z,t) = T_{\text{cond}}(z,t)+\Theta_0(z,t) + \frac{1}{a^2H}\Theta(z,t)\cos ax, \tag{10}$$

with associated expansions for u and p. It is to be noted that the temperature field Θ_0 independent of x includes the modification of the mean temperature distribution by convection. Substituting these expansions in the governing equations and removing horizontal dependence by taking appropriate inner products, we obtain the following partial differential equations for the Fourier amplitudes $W(z,t)$, $\Theta_0(z,t)$ and $\Theta(z,t)$:

$$\frac{\partial}{\partial t}LW = Pr(L^2W-\Theta-f), \tag{11}$$

$$\frac{\partial}{\partial t}\Theta = L\Theta-a^2H(DT_{\text{cond}}+D\Theta_0)W \tag{12}$$

$$\frac{\partial}{\partial t}\Theta_0 = D^2\Theta_0-\frac{1}{2a^2H}D(W\Theta), \tag{13}$$

where $D=\partial/\partial z$, $L=D^2-a^2$ and the random forcing term $f(z,t)$ is

$$f(z,t)=\frac{a^2}{\pi}\int_0^{2\pi/a}\left\{\left(\frac{\partial^2 s_{xx}}{\partial x\,\partial z}+\frac{\partial^2 s_{xz}}{\partial z^2}\right) -\left(\frac{\partial^2 s_{zx}}{\partial x^2}+\frac{\partial^2 s_{zz}}{\partial z\,\partial x}\right)\right\}\sin ax\,\mathrm{d}x. \tag{14}$$

Boundary conditions (5) become

$$\begin{aligned} &W = DW = D\Theta = D\Theta_0 = 0 \quad \text{at} \quad z=0,\\ &W = DW = \Theta = \Theta_0 = 0 \qquad \text{at} \quad z=1. \end{aligned} \tag{15}$$

We seek the solution of (11)–(13) by expanding the variables in terms of eigenfunctions which satisfy

$$L^3\phi_n+\lambda_n^6\phi_n = 0 \quad \text{for} \quad 0<z<1, \tag{16}$$

with boundary conditions

$$\begin{aligned} &\phi_n = D\phi_n = DL^2\phi_n = \quad \text{at} \quad z=0,\\ &\phi_n = D\phi_n = L^2\phi_n = 0 \quad \text{at} \quad z=1. \end{aligned} \tag{17}$$

The eigenfunctions defined by (16) and (17) are those of linear instability of stationary Rayleigh–Bénard convection with a rigid insulating lower boundary and a rigid conducting upper boundary [17]. An explicit expression for the eigenfunction ϕ_n is given in the Appendix. Normalized eigenfunctions satisfy the following orthogonality relation:

$$\int_0^1 \phi_m\cdot L^2\phi_n\,\mathrm{d}z = \delta_{mn}. \tag{18}$$

The Fourier amplitudes $W(a,t)$, $\Theta(z,t)$ and $\Theta_0(z,t)$ are expanded in the following forms:

$$W(z,t) = \sum_{n=1}^{\infty} a_n(t)\phi_n(z), \tag{19}$$

$$\Theta(z,t) = \sum_{n=1}^{\infty} b_n(t)L^2\phi_n(z), \tag{20}$$

$$\Theta_0(z,t) = \sum_{n=1}^{\infty} c_n(t)\cos\left(n-\frac{1}{2}\right)\pi z. \tag{21}$$

Expressions (19)–(21) automatically satisfy boundary conditions (15). By substituting equations (19)–(21) and (8) into equations (11)–(13), taking appropriate inner products and using orthogonality relations (18), we obtain the following infinite set of coupled ordinary random differential equations:

$$\frac{1}{Pr}\frac{\mathrm{d}}{\mathrm{d}t}a_m = \sum_{n=1}^{\infty} A_{mn}(b_n-a_n+f_n), \tag{22}$$

$$\frac{\mathrm{d}}{\mathrm{d}t}b_m = \sum_{n=1}^{\infty}\left\{B_{mn}(Ha_n-H_nb_n)+Ha_n\sum_{l=1}^{\infty} I^l_{mn}(c_l-d_l)\right\}, \tag{23}$$

$$\frac{\mathrm{d}}{\mathrm{d}t}c_m = -\mu_m^2c_m-\frac{1}{H}\sum_{n=1}^{\infty}\sum_{l=1}^{\infty} J^m_{nl}a_nb_l, \tag{24}$$

where A_{mn} is the mn-element of inverse of matrix (C_{mn}) and

$$\begin{aligned} f_n(t) &= \int_0^1 f(z,t)\phi_n(z)\,\mathrm{d}z,\\ H_n &= \lambda_n^6/a^2,\\ d_l(t) &= 2\mathrm{e}^{-\mu_l^2t}/\mu_l^2,\\ B_{mn} &= a^2\int_0^1 \phi_m(z)\phi_n(z)\,\mathrm{d}z,\\ C_{mn} &= -\int_0^1 L\phi_m(z)\phi_n(z)\,\mathrm{d}z,\\ I^l_{mn} &= a^2\mu_l\int_0^1 \phi_m(z)\phi_n(z)\sin\mu_l z\,\mathrm{d}z,\\ J^m_{nl} &= \frac{\mu_m}{a^2}\int_0^1 \phi_n(z)L^2\phi_l(z)\sin\mu_m z\,\mathrm{d}z. \end{aligned} \tag{25}$$

Explicit expressions of B_{mn}, C_{mn}, I^l_{mn} and J^l_{mn} are given in the Appendix. It is to be noted that H_1 takes its minimum value of the stationary critical Rayleigh number R_{sc} $(=1295.78)$ for $a=2.55$ which is the stationary critical wave number a_{sc} [17]. The random

forcing term $f_n(t)$ is a Gaussian process with vanishing mean and its correlation is obtained by use of the relations (4), (14) and (18):

$$\langle f_m(t_1) f_n(t_2)\rangle = 2D_{mn}\delta(t_2 - t_1), \tag{26}$$

where

$$D_{mn} = \varepsilon\delta_{mn}, \quad \varepsilon = Pr\, a^3\theta/\pi. \tag{27}$$

In order to obtain the solutions of the evolution equations (22)–(24), we need the initial conditions for $a_m(t)$, $b_m(t)$ and $c_m(t)$. We consider the initial state of the fluid layer as motionless and pseudo-thermal equilibrium at some average temperature [8]. The initial conditions for b_m and c_m are $b_m(0) = c_m(0) = 0$, since the thermal fluctuations are negligible. On the other hand $a_m(0)$ is related to the statistics of random forcing, and is given by the steady-state solution of (22) with $b_m \equiv 0$:

$$\frac{1}{Pr}\frac{\mathrm{d}}{\mathrm{d}t} a_m = \sum_{n=1}^{\infty} A_{mn}(-a_n + f_n). \tag{28}$$

Equation (28) is a linear Ito equation, and implies that $a_m(t)$ is also a Gaussian process with vanishing mean and its variance for steady state has the following form:

$$\langle a_m a_n\rangle = \varepsilon\, Pr\, A_{mn}.$$

In summary, initial conditions for (22)–(24) are given by

$$\begin{aligned} \langle a_m(0)\rangle &= 0, \\ \langle a_m(0) a_n(0)\rangle &= \varepsilon\, Pr\, A_{mn}, \\ b_m(0) &= c_m(0) = 0. \end{aligned} \tag{29}$$

3. SOLUTION

The random evolution equations (22)–(24) are solved numerically by a Monte Carlo simulation. Each of the series a_m, b_m and c_m has been truncated to a finite number of terms, as required for convergence. The number of terms retained depends on the parameters of the problem. Numerical calculations show that expressions (19)–(21) work more efficiently as the heat flux H decreases, and near the stationary critical Rayleigh number only two or three eigenfunctions are needed for the convergence.

For numerical calculations, it is convenient to represent the white component of $f_n(t)$ in (22) as $\mathrm{d}B_n(t)/\mathrm{d}t$, where $B_n(t)$ is the Wiener or Brownian motion process. The random increment of $B_n(t_2) - B_n(t_1)$ is Gaussian distributed with statistics [18]:

$$\begin{aligned} \langle B_n(t_2) - B_n(t_1)\rangle &= 0, \\ \langle\{B_m(t_2) - B_m(t_1)\}\{B_n(t_2) - B_n(t_1)\}\rangle &= 2D_{mn}|t_2 - t_1|. \end{aligned} \tag{30}$$

The random initial conditions and random increments of forcing terms are generated numerically under the condition that each of them is Gaussian distributed with a vanishing mean and its covariance satisfies relations (26) or (30). For this generation, we have used a polar method of pseudo-random-number generation [19]. For each time step, variables are first integrated deterministically using standard initial value techniques. Next, the randomly generated increments of forcing terms are added to complete the integration.

One of the most widely used methods for the detection of the onset of thermal instability is to measure the heat transport across the fluid layer. At the onset of instability, the heat transport starts to depart from that due to conduction. To express the heat transport, it is convenient to introduce the following time-dependent Nusselt number [14]:

$$Nu(t) = -\frac{h}{\Delta\tilde{T}(\tilde{t})}\cdot\frac{\partial\tilde{T}}{\partial\tilde{z}}(0,0,\tilde{t}) = \frac{H}{R(t)}. \tag{31}$$

Here R is the time-dependent Rayleigh number based on the mean temperature difference between the lower and upper boundaries $\Delta\tilde{T}$,

$$\begin{aligned} R &= \alpha g\Delta\tilde{T}h^3/\kappa\nu = H\cdot\Delta T(t), \\ \Delta T(t) &= k\Delta\tilde{T}(\tilde{t})/Qh = T_{\mathrm{cond}}(0,t) + \Theta_0(0,t). \end{aligned} \tag{32}$$

Typical behaviours of time evolution of Nu and ΔT are shown in Fig. 1 for $Pr = 7$, $H = 10^4$ and $a = 3.9$. At the initial stage, immediately after the heat flux is applied to the lower surface, conduction is the sole mechanism of heat transfer and, therefore, Nu decreases and ΔT increases monotonically with time for a given H. If the convective motion did not occur, both Nu and ΔT would have approached unity which is the value of the conductive steady state. As shown in Fig. 1, however, Nu attains a local minimum at a certain instant t_c and approaches a constant value other than unity after showing transient behaviour. This may be explained by the occurrence of convection. We may define, therefore, the onset time as the ensemble average of the time at which Nu starts to grow for the first time. For the determination of the onset time, wavenumber dependency is removed by choosing the particular wavenumber for which Nu grows fastest.

Although the onset time decreases with the increase of the value of θ, the onset time is rather insensitive to the variation of θ as shown in Fig. 1. For numerical calculations, we have chosen θ as 10^{-6} which is some three orders of magnitude larger than the intensity of the thermodynamic fluctuations in typical fluids [13].

4. RESULTS

The onset time depends on various parameters of the problem. In Fig. 2 the numerical results are shown in graphs of the onset time t_c vs the dimensionless heat flux H for three typical Prandtl numbers 0.7, 7 and 45. Figure 2 also shows the experimental data of Nielsen and Sabersky [14] for $Pr = 45$. Results of numerical calculation are in good agreement with those of experimental observation. It is seen that the onset time increases rapidly as the heat flux H decreases and goes towards infinity when H approaches the limiting value R_{sc} ($= 1296$). When H is lowered below R_{sc}, the fluid layer is stable even in the time-dependent situation. For

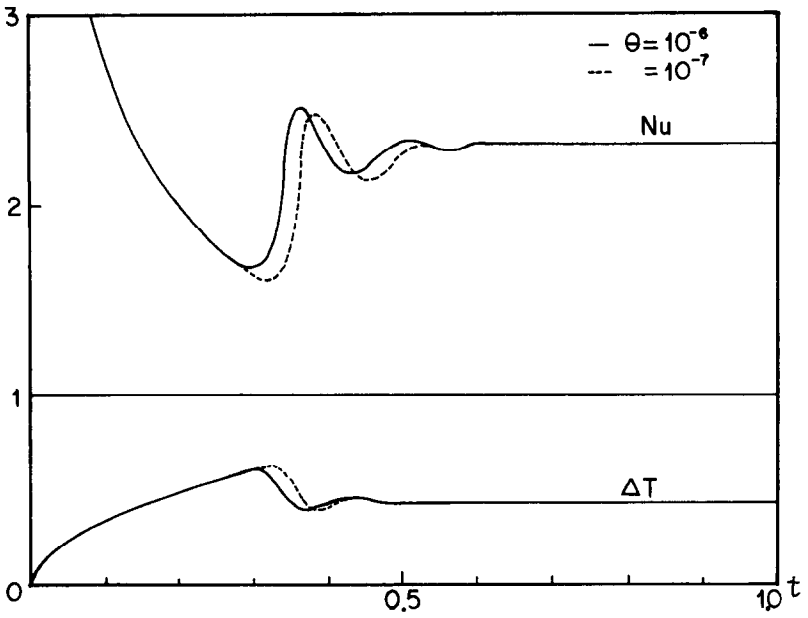

FIG. 1. Behaviour of time-dependent Nusselt number Nu and temperature difference ΔT between the plates for $H = 10^4$, $Pr = 7$ and $a = 3.9$.

very high heat flux, it is known that the depth of fluid should no longer have an influence on the onset time, because instability occurs before the effects of heating have penetrated the fluid layer to the full depth. In this case, the dimensional analysis shows that the dimensionless onset time should be inversely proportional to the square root of H [14]. The proportionality constant is a function of the Prandtl number:

$$H^{1/2}t_c = F(Pr) \quad \text{as} \quad H \to \infty.$$

For $Pr = 45$, numerical calculation gives $H^{1/2}t_c \simeq 20$, while experimental data $H^{1/2}t_c \simeq 19$. Figure 2 shows that each of the shapes of the curves tends towards such a value.

Figure 3 represents plots of the critical Rayleigh number R_c vs the dimensionless heat flux H; as H increases, R_c increases. Increase of Pr results in decrease of R_c for given H. For low heat flux, R_c approaches H independently of the Prandtl numbers. For very high heat flux R_c should be proportional to $H^{3/4}$ or inversely proportional to $t_c^{3/2}$, following arguments similar to those presented above. Each of these trends of the data in Fig. 3 indicates this kind of relationship. The values of analytically predicted critical Rayleigh numbers are 20–30% larger than those observed, while theoretical values of onset times show good agreement with observations. A probable explanation for this difference is that in the analysis, the critical Rayleigh

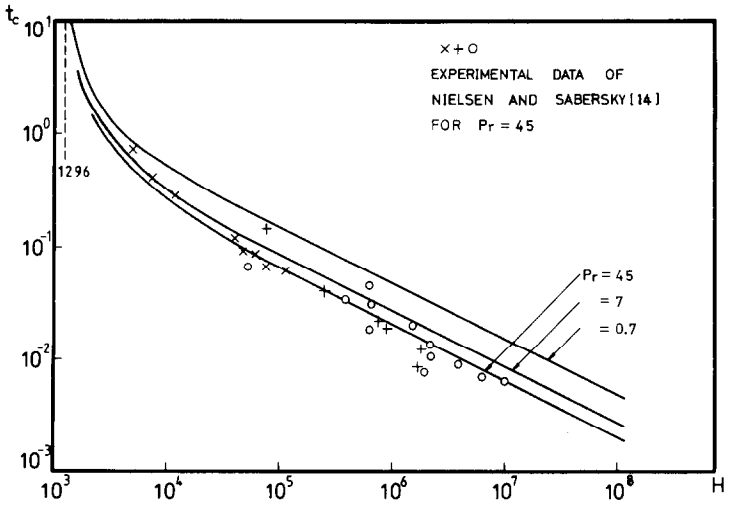

FIG. 2. Onset time t_c plotted as a function of dimensionless heat flux H.

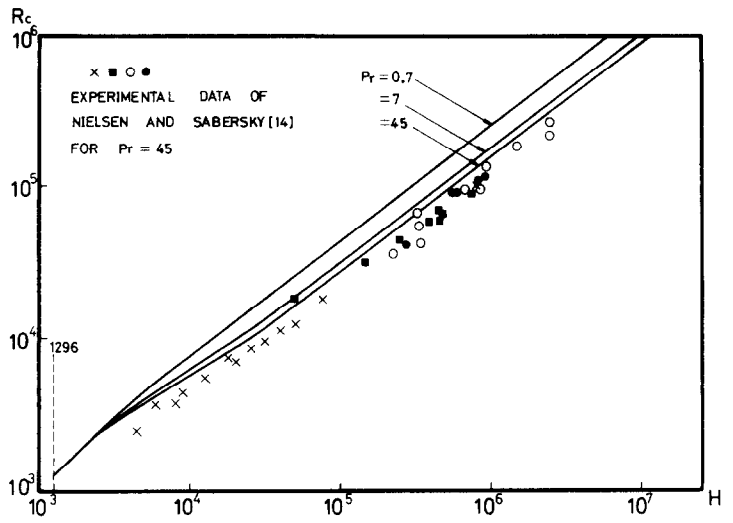

FIG. 3. Critical Rayleigh number R_c plotted against dimensionless heat flux H.

number is defined with the temperature difference ΔT at the instant at which the temperature difference begins to deviate from that solely due to conduction, whereas in an experiment ΔT might have been measured at an instant shortly after the motion actually started. Because of the rapid variation of the temperature difference during a period after the onset time as shown in Fig. 1, a small time discrepancy can result in a significant decrease of the temperature difference or critical Rayleigh number.

In Fig. 4 the critical Nusselt number Nu_c is plotted against the critical Rayleigh number R_c. It is seen that Nu_c increases as R_c or Pr increases. For low heat flux Nu_c decreases towards unity as R_c decreases. For very high heat flux Nu_c becomes proportional to $R_c^{1/3}$. As indicated in Fig. 4, each of the curves approaches the slope as expected. The transient critical wave number a_c at which Nu grows fastest increases with the heat flux H. For low heat flux, a_c approaches the stationary critical wavenumber a_{sc} ($=2.55$). While for high heat flux, a_c should be proportional to $H^{1/4}$. This tendency can be confirmed (Fig. 5).

Taken together, Figs. 2–5 indicate that as the heat flux is increased for a fixed Prandtl number, the onset time decreases while the critical Rayleigh number, the critical Nusselt number and the critical wavenumber increase; as the Prandtl number is increased for a fixed heat flux, the onset time and the critical Rayleigh number decrease while the critical Nusselt number increases. These trends are in agreement with both theoretical predictions using frozen time analysis by Currie [2] and experimental data of Nielsen and Sabersky [14]. However, values of the onset times in the present analysis agree well with those observed not only qualitatively but also quantitatively, while Currie's values are significantly shorter than those observed.

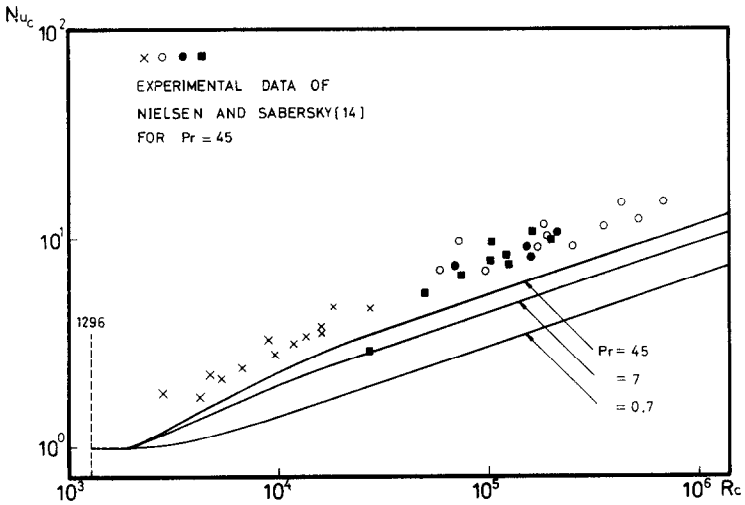

FIG. 4. Critical time-dependent Nusselt number Nu_c plotted against critical Rayleigh number R_c.

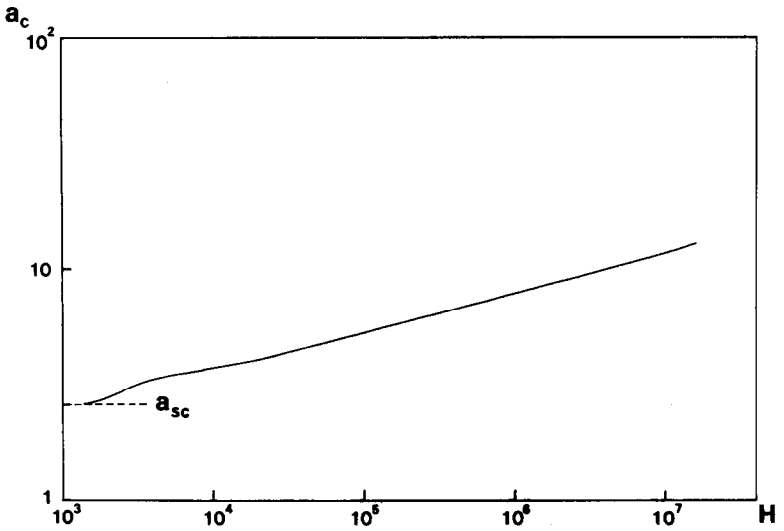

FIG. 5. Critical wave number a_c plotted against heat flux H for $Pr = 0.7$.

5. SUMMARY AND DISCUSSIONS

The onset of convection in a fluid layer bounded by rigid surfaces and subject to a time-dependent profile by a constant heat flux from below has been considered with the inclusion of random fluctuations. The dependency of the onset time (defined as the ensemble mean of the time at which the bottom-surface temperature starts to decrease for the first time) on the heat flux was established. The results show that the onset time decreases as the Prandtl number, the heat flux or the Rayleigh number increases; the results agree quantitatively with the experimental data.

For very high heat flux, $R_c t_c^{3/2}$ approaches an asymptote, which is a function of the Prandtl number. This asymptote is about 2450 for $Pr = 0.7$, 740 for $Pr = 7$ and 460 for $Pr = 45$, respectively. Compared with the experimental results of Davenport and King [15] or the numerical results of the present authors [9], this asymptote for a fixed Prandtl number is higher than that for the case of step change but lower than that for the case of linear change in surface temperature. The onset time depends, in general, on the method of time-dependent heating or boundary conditions as well as the heating rate. A simple factor indicating the method of heating is the shape factor s defined as [15]

$$s = \int_0^{t_c} \Delta T(t)\,\mathrm{d}t / \Delta T(t_c) \cdot t_c.$$

By this definition, $s = 1$ for the step change and $s = 1/2$ for the linear change in surface temperature, while for fixed heat flux s falls in the range $0.5 < s < 1$. The results obtained in this work are in agreement with the fact that the asymptote for high heating rate decreases with increase in s [9, 15].

REFERENCES

1. W. Lick, The instability of a fluid layer with time-dependent heating, *J. Fluid Mech.* **21**, 565–576 (1965).
2. I. G. Currie, The effect of heating rate on the stability of stationary fluids, *J. Fluid Mech.* **29**, 337–347 (1967).
3. G. M. Homsy, Global stability of time-dependent flows: impulsively heated or cooled fluid layers, *J. Fluid Mech.* **60**, 129–139 (1973).
4. P. C. Wankat and G. M. Homsy, Lower bounds for the onset time of instability in heated layers, *Phys. Fluids* **20**, 1200–1201 (1977).
5. T. D. Foster, Stability of a homogeneous fluid cooled uniformly from above, *Phys. Fluids* **8**, 1249–1257 (1965).
6. P. M. Gresho and R. L. Sani, The stability of a fluid layer subjected to a step change in temperature: transient vs frozen time analysis, *Int. J. Heat Mass Transfer* **14**, 207–221 (1971).
7. M. Kaviany, The onset of thermal convection in a fluid layer with time-dependent temperature distribution, *Int. J. Heat Mass Transfer* **27**, 375–381 (1984).
8. B. S. Jhaveri and G. M. Homsy, The onset of convection in fluid layers heated rapidly in a time-dependent manner, *J. Fluid Mech.* **114**, 251–260 (1982).
9. K.-H. Kim and M.-U. Kim, Effect of time-dependent heating on the onset of Rayleigh–Bénard convection, *J. phys. Soc. Jap.* **54**, 933–941 (1985).
10. R. K. Soberman, Onset of convection in liquids subjected to transient heating from below, *Phys. Fluids* **2**, 131–138 (1959).
11. T. D. Foster, Onset of manifest convection in a layer of fluid with a time-dependent temperature profile, *Phys. Fluids* **12**, 2482–2487 (1969).
12. L. M. Blair and J. A. Quinn, The onset of cellular convection in a fluid layer with time-dependent density gradients, *J. Fluid Mech.* **36**, 385–400 (1969).
13. E. G. Mahler and R. S. Schechter, The stability of a fluid layer with gas absorption, *Chem. Engng Sci.* **25**, 955–968 (1970).
14. R. C. Nielsen and R. H. Sabersky, Transient heat transfer in Bénard convection, *Int. J. Heat Mass Transfer* **16**, 2407–2420 (1973).
15. I. F. Davenport and C. J. King, The onset of natural convection from time-dependent profiles, *Int. J. Heat Mass Transfer* **17**, 69–76 (1974).
16. L. D. Landau and F. M. Lifshitz, *Fluid Mechanics*. Pergamon Press, New York (1959).
17. E. M. Sparrow, R. J. Goldstein and V. K. Jonsson, Thermal instability in a horizontal fluid layer: effect of boundary conditions and nonlinear temperature profile, *J. Fluid Mech.* **18**, 513–528 (1964).
18. T. T. Soong, *Random Differential Equations in Science and Engineering*. Academic Press, New York (1973).

19. D. Knuth, *The Art of Computer Programming*, Vol. 2. Addison-Wesley, Englewood Cliffs, NJ (1969).

APPENDIX

The orthonormal eigenfunction satisfying equations (16)–(18) can be written as:

$$\phi_n(z) = \sum_{p=1}^{2}\sum_{r=1}^{3} d_n^p v_{nr}^p \psi_{nr}^p(z), \tag{A1}$$

where

$$\psi_{nr}^1(z) = \cos\left\{\alpha_{nr}\left(z-\frac{1}{2}\right)\right\}\Big/\cos(\alpha_{nr}/2),$$

$$\psi_{nr}^2(z) = \sin\left\{\alpha_{nr}\left(z-\frac{1}{2}\right)\right\}\Big/\sin(\alpha_{nr}/2),$$

$$\alpha_{n_1} = (\lambda_n^2 - a^2)^{1/2},$$

$$\alpha_{n_2} = \{(\lambda_n^4+\lambda_n^2a^2+a^4)^{1/2}/2-(\lambda_n^2+a^2/2)/2\}^{1/2} + i\{(\lambda_n^4+\lambda_n^2a^2+a^4)^{1/2}/2+(\lambda_n^2+a^2/2)/2\}^{1/2},$$

$$\alpha_{n_3} = \alpha_{n_2}^*,$$

$$c_1 = 1,\ c_2 = c,\ c_3 = c^*,\ c = \exp(-2i\pi/3),$$

$$\eta_{nr}^1 = +\alpha_{nr}\tan(\alpha_{nr}/2),$$

$$\eta_{nr}^2 = -\alpha_{nr}\cot(\alpha_{nr}/2),$$

$$\xi_n^p = [\beta_{n_1}^p - \mathrm{Re}(\eta_{n_2}^p)]/2\,\mathrm{Im}(\eta_{n_2}^p),$$

$$v_{n_1}^p = 1,\ v_{n_2}^p = -\frac{1}{2}+i\xi_n^p,\ v_{n_3}^p = v_{n_2}^{p*},$$

$$\gamma_{nr}^p = v_{nr}^p\{\alpha_{nr}^2+2\eta_{nr}^p+(\eta_{nr}^p)^2\}/2\alpha_{nr}^2,$$

$$\beta_{nr}^p = v_{nr}^p\eta_{nr}^p,$$

$$g_n = \left[\sum_{p=1}^{2}\sum_{r=1}^{3}\frac{c_r\gamma_{nr}^p}{\lambda_n^4(\xi_n^p+\sqrt{3}/2)^2}\right]^{-1/2},$$

$$d_n^p = (-1)^{p-1}g_n\Big/\left(\xi_n^p+\frac{\sqrt{3}}{2}\right),$$

and the eigenvalue λ_n is determined to satisfy the following equation:

$$\sum_{p=1}^{2}\sum_{r=1}^{3}\frac{1}{\xi_n^p+\sqrt{3}/2}\,\mathrm{Im}(c_p^*\beta_{nr}^p) = 0.$$

For a fixed wavenumber, the asymptotic behaviour of eigenvalue λ_n for large n is given by

$$\lambda_n \sim \left\{a^2+\left(n+\frac{1}{6}\right)^2\pi^2\right\}^{1/2} \quad \text{as} \quad n\to\infty.$$

Using Newton's method with above relation as an initial value for λ_n, we can easily calculate the accurate eigenvalue λ_n. Differentiating (A1), $L\phi_n$ and $L^2\phi_n$ are written as

$$L\phi_n(z) = -\lambda_n^2\sum_{p=1}^{2}\sum_{r=1}^{3} d_n^p c_r^* v_{nr}^p\psi_{nr}^p(z)$$

$$L^2\phi_n(z) = +\lambda_n^4\sum_{p=1}^{3}\sum_{r=1}^{3} d_n^p c_r v_{nr}^p\psi_{nr}^p(z).$$

Making use of these results, B_{mn}, C_{mn}, I_{mn}^l and J_{mn}^l are obtained after straightforward calculations:

$$B_{mn} = a^2\sum_{p=1}^{2}\sum_{r=1}^{3}(d_n^p)^2 v_{nr}^p\gamma_{nr}^p, \quad \text{if } m=n$$

$$= \frac{12a^2\lambda_m^2\lambda_n^2}{\lambda_m^6-\lambda_n^6}\sum_{p=1}^{2} d_m^p d_n^p\left\{\left(\xi_n^p-\frac{\sqrt{3}}{2}\right)\mathrm{Im}(c\beta_{m_2}^p) - \left(\xi_m^p-\frac{\sqrt{3}}{2}\right)\mathrm{Im}(c\beta_{n_2}^p)\right\}, \quad \text{if } m\neq n$$

$$C_{mn} = \sum_{p=1}^{2}\left[\left\{\lambda_n^2(d_n^p)^2\sum_{r=1}^{3} c_r^* v_{nr}^p\gamma_{nr}^p\right\} - 4\sqrt{3}\,\mathrm{Im}(\gamma_{n_2}^{p*}\beta_{n_2}^p)\right], \quad \text{if } m=n$$

$$= \frac{12\lambda_m^2\lambda_n^2}{\lambda_m^6-\lambda_n^6}\,\mathrm{Im}\sum_{p=1}^{2}\left[\left\{\left(\xi_n^p-\frac{\sqrt{3}}{2}\right)\lambda_m^2c^* + \left(\xi_n^p+\frac{\sqrt{3}}{2}\right)\lambda_n^2c\right\}\beta_{n_2}^p - \left\{\left(\xi_m^p-\frac{\sqrt{3}}{2}\right)\lambda_n^2c^* + \left(\xi_m^p+\frac{\sqrt{3}}{2}\right)\lambda_m^2c\right\}\beta_{m_2}^p\right], \quad \text{if } m\neq n$$

$$I_{mn}^l = a^2\sum_{r=1}^{3}\sum_{s=1}^{3}\sigma_{mnlrs},$$

$$J_{mn}^l = \frac{\lambda_n^4}{a^2}\sum_{r=1}^{3}\sum_{s=1}^{3} c_s\sigma_{mnlrs},$$

where

$$\sigma_{mnlrs} = \frac{\gamma}{\gamma^4-2\gamma^2(\alpha_{mr}^2+\alpha_{ns}^2)+(\alpha_{mr}^2-\alpha_{ns}^2)^2} \times[(-1)^l\{(\gamma^2-\alpha_{mr}^2+\alpha_{ns}^2)(\mu_{ns}^1+\mu_{ns}^2)(\mu_{mr}^1\eta_{mr}^1+\mu_{mr}^2\eta_{mr}^2) + (\gamma^2-\alpha_{ns}^2+\alpha_{mr}^2)(\mu_{mr}^1+\mu_{mr}^2)(\mu_{ns}^1\eta_{ns}^1+\mu_{ns}^2\eta_{ns}^2)\} + \gamma\{(\gamma^2-\alpha_{mr}^2-\alpha_{ns}^2)(\mu_{mr}^1-\mu_{mr}^2)(\mu_{ns}^1-\mu_{ns}^2) - 2(\mu_{mr}^1\eta_{mr}^1-\mu_{mr}^2\eta_{mr}^2)(\mu_{ns}^1\eta_{ns}^1-\mu_{ns}^2\eta_{ns}^2)\}],$$

$$\gamma = \left(l-\frac{1}{2}\right)\pi, \quad \mu_{mr}^p = d_m^p v_{mr}^p.$$

APPARITION DE CONVECTION NATURELLE DANS UNE COUCHE DE FLUIDE BRUSQUEMENT CHAUFFEE PAR DESSOUS

Résumé—L'apparition de convection dans une couche de fluide, dans laquelle le profil de température varie dans le temps, est considérée avec inclusion de fluctuations désordonnées lorsqu'un flux thermique constant est brusquement appliqué à la surface inférieure. Utilisant un développement en fonctions propres de l'instabilité linéaire, les équations sont réduites en un système d'équations différentielles qui sont résolues par un simulation Monte Carlo. On étudie la dépendance du temps d'apparition de la convection vis-à-vis du nombre de Rayleigh et du nombre de Prandtl. Les résultats numériques sont en bon accord avec les données expérimentales disponibles.

EINSETZEN DER NATÜRLICHEN KONVEKTION IN EINER FLUIDSCHICHT BEI PLÖTZLICHER ERWÄRMUNG VON UNTEN

Zusammenfassung—Es wird das Einsetzen der Konvektion in einer Fluidschicht bei zeitlicher Veränderung des Temperaturprofils unter Berücksichtigung von zufälligen Schwankungen betrachtet, wenn plötzlich ein konstanter Wärmestrom an der Bodenfläche aufgebracht wird. Die geltenden Gleichungen werden mit Hilfe der Eigenfunktionen der linearen Instabilität auf einen Satz von normalen Zufallsdifferentialgleichungen zurückgeführt, welcher mit Hilfe einer Monte-Carlo-Simulation gelöst wird. Die Abhängigkeit des Zeitpunktes des Einsetzens der Konvektion von der Rayleigh-Zahl und der Prandtl-Zahl wird untersucht. Die numerischen Eegebnisse stimmen gut mit den verfügbaren experimentellen Daten überein.

ВОЗНИКНОВЕНИЕ ЕСТЕСТВЕННОЙ КОНВЕКЦИИ В СЛОЕ ЖИДКОСТИ В УСЛОВИЯХ МГНОВЕННОГО НАГРЕВА СНИЗУ

Аннотация—Рассматривается возникновение конвекции в слое жидкости, в котором температурный профиль развивается во времени с учетом случайных флуктуаций, когда постоянным тепловым потоком внезапно начинает разогреваться нижняя поверхность. При использовании разложения по собственным функциям в линейной задаче устойчивости определяющие уравнения сводятся к системе обыкновенных дифференциальных уравнений, которые решаются методом Монте-Карло. Исследуется зависимость времени возникновения конвекции от чисел Рэлея и Прандтля. Численные результаты хорошо согласуются с имеющимися экспериментальными данными.